Fluids in the system forsterite-phlogopite-H2O at 60 kbar

Autor(en): **Stalder, Roland / Ulmer, Peter / Günther, Detlef**

Objekttyp: **Article**

Zeitschrift: **Schweizerische mineralogische und petrographische Mitteilungen = Bulletin suisse de minéralogie et pétrographie**

Band (Jahr): **82 (2002)**

Heft 1

PDF erstellt am: **26.09.2024**

Persistenter Link: https://doi.org/10.5169/seals-62349

SCHWEIZ. MINERAL. PETROGR. MITT. 82, 15–24, 2002

Fluids in the system forsterite–phlogopite–H_2O at 60 kbar

by *Roland Stalder*[1*], *Peter Ulmer*[1] and *Detlef Günther*[2]

Abstract

A series of high-pressure experiments in the KMASH-system (K_2O–MgO–Al_2O_3–SiO_2–H_2O) has been performed to constrain the compositions of potential K-rich metasomatic agents under upper mantle conditions in equilibrium with phlogopite. Two sets of experiments were conducted, one on the join phlogopite–H_2O and a second one in the system forsterite–phlogopite–H_2O. Experiments were performed at 60 kbar and 800 to 1200 °C in a Walker-type multi-anvil press. Fluids or melts were trapped in a diamond layer that was added to the experimental charge as a layer separated from the silicate phases. Traps were analysed by laser ablation-ICP-MS, and residues were inspected by micro-Raman spectroscopy and laser ablation-ICP-MS.

Fluid compositions do not vary strongly with temperature, and runs performed in the system forsterite–phlogopite–H_2O show similar results to runs conducted in the initially forsterite-free system. The quench-products of all fluids exhibit a composition that is slightly more potassic and slightly poorer in silica than phlogopite, and the Al-contents closely match that of phlogopite. In all cases garnet is formed upon phlogopite dissolution. In runs, which initially did not contain forsterite, forsterite was detected at temperatures in excess of 1000 °C. The total amount of dissolved silicate was probably around or higher than 50 wt% under all run conditions.

Keywords: High pressure, fluid phase, phlogopite, metasomatism.

1. Introduction

Phlogopite is an important carrier of H_2O and K_2O in the upper mantle, and the system forsterite–phlogopite–H_2O can be regarded as a simple model system for K-metasomatism in the Earth's mantle. Well-known examples of modal K-rich mantle metasomatism are the occurrence of phlogopite peridotites (PP) and phlogopite – K-richterite peridotites (PKP) (AOKI, 1975; ERLANK et al., 1987; WATERS and ERLANK, 1988) as well as the MARID (Mica–Amphibole–Rutile–Ilmenite–Diopside) nodules that occur as xenoliths in kimberlites (DAWSON and SMITH, 1977). As one possible mechanism for the generation of phlogopite and K-richterite bearing peridotites and MARID assemblages the reaction of hydrous alkali-rich fluids/melts with "ordinary" mantle peridotite has been proposed (AOKI, 1975; ERLANK et al., 1987; SWEENEY et al., 1993).

In an H_2O saturated lherzolite between 10 and 30 kbar phlogopite decomposes at the solidus by the reaction orthopyroxene + clinopyroxene + phlogopite + fluid → olivine + spinel/garnet + melt, whereby the melt in equilibrium with enstatite, forsterite and phlogopite becomes more alkalic and more SiO_2-undersaturated with increasing pressure (MODRESKY and BOETTCHER, 1973). Under H_2O-saturated conditions the melting temperature of phlogopite up to 35 kbar is lowered considerably by the presence of enstatite (MODRESKY and BOETTCHER, 1972). At the solidus, phlogopite is not consumed totally, suggesting that dehydration melting is not the appropriate process. In a more complex lherzolitic system with mixed CHO-fluids, phlogopite is stable at the solidus temperature up to 50 kbar (WENDLANDT and EGGLER, 1980). The fluid phase in equilibrium with phlogopite shows incongruent dissolution at low pressure, but increasing amounts of

[1] Institut für Mineralogie und Petrographie, ETH-Zentrum, Sonneggstrasse 5, CH-8092 Zürich, Switzerland.
[*] Present address: Geowissenschaftliches Zentrum der Universität Göttingen, Abteilung Angewandte und Experimentelle Mineralogie, Goldschmidtstraße 1, D-37077 Göttingen, Germany. <rstalde@gwdg.de>
[2] Laboratorium für Anorganische Chemie, ETH-Zentrum, Universitätsstrasse 6, CH-8092 Zürich, Switzerland.

quench phlogopite are observed at pressures up to 30 kbar (YODER and KUSHIRO, 1969; RYABCHIKOV and BOETTCHER, 1980). Furthermore, excessive amounts of potassium in the fluid phase have been observed (RYABCHIKOV and BOETTCHER, 1980).

Beside many studies in the system forsterite–phlogopite–water and in the KMASH system in general, quantitative data concerning the composition of the fluid phase are only determined up to 20 kbar (RYABCHIKOV and BOETTCHER, 1980; SCHNEIDER and EGGLER, 1986). Therefore the present study was designed to investigate the chemical composition of aqueous fluids saturated with phlogopite and lherzolite phases at pressures relevant for the generation of ultrapotassic rocks and the inferred conditions for K-rich mantle metasomatism observed in cratonic lithospheric mantle, i.e. at pressures up to 60 kbar (some 200 km depth) (SATO et al., 1997).

2. Experimental

The composition of the starting material has to meet the prerequisite that the fluid composition is buffered, i. e. in a 5-component system (K_2O–MgO–Al_2O_3–SiO_2–H_2O) 5 phases have to be present. Due to high K-solubilities in the fluid phase and a positive correlation between K-solubility and pressure (RYABCHIKOV and BOETTCHER, 1980) the production of garnet upon phlogopite dissolution was anticipated. Furthermore, a high MgO-content in the fluid under ambient pressure was expected (RYABCHIKOV and BOETTCHER, 1980; STALDER et al., 2001), leaving enstatite (rather than forsterite) in the solid residue. Therefore, two sets of experiments were conducted, one on the join phlogopite–H_2O and a second one in the system forsterite–phlogopite–H_2O, expecting that the existing phases were not consumed and additional solid residual phases (3 or 2, respectively) will be produced, and saturate the fluid in all components. As starting materials two mixtures corresponding to the respective stoichiometric compositions of phlogopite and forsterite were prepared from oxides; potassium was added as K_2CO_3. These stoichiometric mixture were sealed with some excess water in Au-capsule with an OD(ID) of 5.0 (4.4) mm and about 20 mm length. They were run for 260 hours at 1.5 kbar and 700 °C in a cold-sealed hydrothermal vessel. After the runs the capsules were weighed, pierced, dried at 120 °C, and weighed again; the weight loss upon piercing matched the CO_2 content of the starting mixture. The dried products were inspected by powder X-ray diffraction. They contained phlogopite + glass (approximately 30:70 wt%) and forsterite (and minor amounts of talc and periclase), respectively. The incomplete synthesis yield was not regarded as a problem, as the main purpose of the synthesis procedure was the homogeneous dissemination of the K_2O in the starting material. The synthesis products were quantitatively recovered and re-homogenised. Apart from the amount of water the compositions of the synthesis products are not affected by the incomplete synthesis yield. The bulk composition of the first set of experiments corresponded to 85 wt% phlogopite and 15 wt% H_2O, the second set contained a mixture of equal amounts of both syntheses (forsterite + phlogopite) and 15 wt% H_2O. For each run 10 mg starting mixture and 1.5 mg H_2O were sealed in an Au-capsule with an outer (inner) diameter of 2.3 (2.0) mm. A layer consisting of 3 mg diamonds (grain size 20 mm) was added to all charges, except KMASH1 and KMASH2. In order to optimise the geometry, an Au-ring with an outer (inner) diameter of 1.8 (1.5) mm was inserted into the Au-capsule (STALDER et al., 2001). The pore space between the diamonds stays open during the entire run time and upon quenching the fluid or hydrous melt can be separated from the solid residue. The application of the diamond trap technique implies that CO_2 may have been present during run conditions in minor amounts ($X\ CO_2 << 0.1$) due to reactions with the trap diamonds, but deviations of the results from those of the CO_2-absent system are expected to be small (STALDER et al., 2000).

Experiments were performed at 60 kbar between 800 and 1200 °C in a Walker-type multi-anvil press. Temperatures were measured with a Pt–$Pt_{90}Rh_{10}$ thermocouple; no pressure correction

Table 1 Run details and phase assemblages.

Run	P (kbar)	T (°C)	Time (hours)	Phase assemblages
System Phlogopite-H_2O				
KMASH2	60	800	8	Gt,Phl, (En)
KMASH 15	60	800	24	Gt, Phl
KMASH 6	60	900	24	Gt, Phl
KMASH 10	60	1000	8	Gt, Phl, (Fo)
KMASH 12	60	1100	7	Gt, Phl, (Fo), (En)
KMASH 14	60	1200	2	Gt, Phl, Fo, (En)
System Forsterite-Phlogopite-H_2O				
KMASH1	60	800	5	Fo,Gt, Phl
KMASH 5	60	900	24	Fo, Gt, Phl
KMASH 9	60	1000	8	Fo, Gt, Phl
KMASH 11	60	1100	4	Fo, Gt, (Phl)
KMASH 13	60	1200	2	Fo, Gt

Gt–garnet, Phl–phlogopite, Fo–forsterite, En–enstatite.
( )–phase observed only in minor amounts.

was applied to the EMF. Pressures are estimated to be correct within ±3 kbar and temperatures within less than ±20 °C. Run times were between 2 and 24 hours depending on temperature (Table 1). After the runs charges were weighed, pierced, dried, and weighed again. In all runs reported here an aqueous solution visibly escaped upon piercing. Capsules were embedded in epoxy and manually ground until their maximum cross section was exposed. Four to six points with a spot size of 120 µm were analysed on each trap by laser ablation-inductively coupled plasma mass spectrometry (LA-ICP-MS). An 193 ArF excimer laser (Lambda Physik, Göttingen, Germany) was coupled to a Perkin Elmer Elan 6100 DRC ICP-MS (GÜNTHER et al., 1997; HATTENDORF and GÜNTHER, 2000). The laser flux was adjusted to 20 J/cm^2, and a beam diameter of 120 µm at a repetition rate of 10 Hz was used for the analysis. Helium admixed with argon was used as carrier gas for the aerosol transport from the ablation cell to the ICP-MS. External calibration was carried out using the glass reference standard 610 from NIST. The data acquisition and data reduction procedure for laser ablation-ICP-MS discribed in LONGERICH et al. (1996) were applied. In the first step we determine element concentrations in the trap relative to each other. These values are then divided by the drift- and background-corrected count-rate for ^{13}C (STALDER et al., 2000). In this way carbon is used as internal standard and the absolute silicate content can be considered to be relatively correct within analytical error from one analysed spot to another (e.g., a higher C/Si count rate means a lower Si-concentration in the trap).

For two runs (KMASH 14 and 15) the pH of the escaping solution was checked by indicator paper. In both cases the solution was highly basic (pH = 14). In most runs – especially those at high temperatures – the weight loss after fluid extraction was significantly higher than the initial amount of water in the capsule. This indicates that the dissolved material in the fluid did not precipitate quantitatively upon quenching, and hence the calculation procedure of STALDER et al. (2000, 2001) to determine the absolute amount of solute content cannot be applied. Hence, all values obtained for solute concentration have to be regarded as relative data. As will be shown in a later section, a different approach (based on the comparison between the chemical analyses of the quenched material and the solution after quenching) has been applied to estimate the total solute content.

All crystalline residues (located in the lower part of the capsule) were inspected by micro-Raman spectroscopy; in addition, the existence of some minerals in the solid residues (especially garnet) was confirmed by laser ablation-ICP-MS. Charges KMASH1 and KMASH2 were merely applied for phase analysis. As they did not contain any diamonds, polishing was possible and detection of small grains was facilitated.

3. Results

Phase assemblages are listed in Table 1. Corresponding to the starting material, phlogopite or forsterite and phlogopite were detected as euhedral grains in nearly all runs. Phlogopite commonly formed large grains; it was only absent in the run at 1200 °C, which initially contained equal amounts of forsterite and phlogopite (KMASH13), where it was consumed totally. In runs on the join phlogopite–H_2O (i.e., with no initial forsterite), forsterite was detected in run products above 1000 °C. In all cases euhedral grains of garnet are observed, formed as an additional residual phase upon phlogopite dissolution. A few Raman-spectra of tiny grains (a few microns in diameter) exhibited some peaks characteristic for enstatite (i.e. at 680 and 1030 cm^{-1}). However, the poor quality of these spectra did not allow an unequivocal identification of enstatite. As will be discussed below, all runs but one (KMASH13) were probably buffered by the same phase assemblage.

The compositions of the dry solutes are summarised in Figs. 1 and 2 and in Table 2. For most runs all measured data points cluster well within a compositional range close to phlogopite. Points that fall far outside 1σ in terms of element ratios and absolute solubility are listed separately in Table 2 as outliers. They all have in common that they show a lower total silicate content and a positive deviation in K-content relative to Mg, Al and Si. Nearly all data-points align closely along a line defined by the composition of phlogopite and a composition consisting of about one third SiO_2 and two thirds K_2O. Relative element concentrations in the fluid do not vary strongly with temperature, and runs performed in the system forsterite–phlogopite–H_2O (Fig. 2) show very similar results as runs conducted in the initially forsterite-free system (Fig. 1). A slight increase in relative K-contents compared to all other elements is observed with increasing temperature; otherwise, no significant trend in terms of element ratios is visible. The only run that shows significant deviations from that array is the run KMASH13 (1200 °C, Fig. 2). This experiment was conducted in the system forsterite–phlogopite–H_2O; it is the only charge, in which no phlogopite was detected in

Table 2 Analytical results from LA-ICP-MS.

Run	T (°C)	points	MgO a.u.	Al_2O_3 a.u.	SiO_2 a.u.	K_2O a.u.	Mg/Si wt.	K/Al wt.	Mg/Al wt.	Si/K wt.	Silicate^{tot} a.u.	excess loss wt%
System Phlogopite-H_2O												
KMASH15	800	3	14.9 (1.6)	4.8 (0.5)	15.4 (2.5)	5.8 (0.7)	0.98 (0.06)	1.21 (0.01)	3.11 (0.02)	2.64 (0.14)	40.9 (5.3)	6
KMASH6	900	4	19.4 (3.8)	7.3 (1.0)	22.6 (3.8)	9.6 (1.6)	0.86 (0.02)	1.32 (0.09)	2.65 (0.16)	2.36 (0.17)	58.8 (10.0)	
KMASH10	1000	4	18.3 (1.9)	6.6 (0.7)	20.3 (2.6)	9.5 (1.4)	0.90 (0.02)	1.43 (0.09)	2.77 (0.02)	2.14 (0.09)	54.8 (6.6)	6
KMASH12	1100	4	9.0 (3.0)	3.6 (0.9)	12.2 (3.5)	7.1 (1.7)	0.74 (0.08)	2.02 (0.23)	2.49 (0.27)	1.69 (0.12)	31.9 (8.8)	20
KMASH14	1200	4	13.0 (4.0)	4.8 (1.0)	13.8 (3.6)	7.8 (1.5)	0.93 (0.06)	1.62 (0.08)	2.65 (0.31)	1.76 (0.15)	39.3 (10.0)	30
outliers:												
KMASH15	800	1	4.2	1.4	4.5	2.2	0.94	1.53	2.94	2.04	12.3	6
KMASH6	900	1	5.9	2.7	7.7	5.8	0.76	2.13	2.16	1.33	22.2	
KMASH10	1000	1	5.3	2.6	6.9	5.0	0.78	1.91	2.06	1.39	19.8	6
KMASH10	1000	1	3.3	1.7	5.3	3.3	0.62	2.01	1.98	1.59	13.5	6
KMASH12	1100	1	3.7	1.4	11.1	9.2	0.33	6.43	2.59	1.21	25.4	20
KMASH12	1100	1	2.8	1.1	6.8	6.7	0.41	6.35	2.59	1.01	17.4	20
KMASH14	1200	1	4.5	2.0	8.0	8.8	0.56	4.39	2.23	0.92	23.3	30
KMASH14	1200	1	4.3	2.1	10.7	16.1	0.40	7.63	2.05	0.67	33.2	30
System Forsterite-Phlogopite-H_2O												
KMASH5	900	5	13.3 (3.3)	5.1 (0.9)	16.8 (2.6)	5.7 (1.0)	0.80 (0.18)	1.10 (0.03)	2.57 (0.42)	2.97 (0.18)	40.9 (7.0)	13
KMASH9	1000	5	19.7 (14.1)	7.5 (5.3)	24.0 (18.0)	10.8 (7.1)	0.83 (0.03)	1.50 (0.16)	2.59 (0.16)	2.11 (0.30)	62.0 (44.4)	17
KMASH11	1100	5	14.5 (3.3)	5.5 (1.0)	16.0 (3.7)	7.3 (1.7)	0.91 (0.02)	1.31 (0.10)	2.61 (0.14)	2.20 (0.17)	43.3 (9.7)	24
KMASH13	1200	2	41.6 (6.9)	0.1 (0.1)	19.6 (3.4)	1.3 (0.8)	2.12 (0.02)	9.87 (0.17)	373 (188)	17.7 (8.5)	62.6 (11.2)	25
KMASH13	1200	3	10.9 (8.9)	1.4 (0.5)	8.9 (2.4)	6.1 (3.0)	1.12 (0.61)	4.16 (0.72)	11 (13)	1.91 (1.53)	27.3 (8.6)	25
outlier:												
KMASH9	1000	1	1.2	0.5	2.8	4.2	0.44	7.74	2.28	0.67	8.7	17

a.u.–arbitrary units; values in ( ) give standard deviation (1σ); outliers are listed separately as single points.

the crystalline residue of the run product. The considerably lower Al-content and the high Mg-content of the quenched solute reflect the total consumption of phlogopite and an increasing amount of a forsteritic component in the non-solid phase (whether it is one or two non-solid phases will be discussed below). The data points with a Mg/Si-ratio bigger than that of forsterite suggest that all analyses are shifted systematically towards lower Si-contents. This is probably due to a small systematic analytical error, as all data points (Figs. 1b, 2b) plot on compositions slightly lower in SiO_2 than phlogopite. If this shift were real, mass balance would require unreasonably high amounts of enstatite in the solid residue (which has not been observed) or an unreasonably high amount of silica in the fluid. Furthermore, it is very unlikely to be generated by incongruent dissolution of forsterite, as the eutectic in the MSH-system at 60 kbar is well between forsterite and enstatite (STALDER et al., 2001).

Most capsules expelled a highly alkaline solution when pierced after the run, and a white cover around the puncturing was exhibited after drying, indicating that solute was present in the hydrous solution after quenching. Capsules showed a significantly higher weight loss than expected from the release of the initial water only. In the following, we will call this "excess weight loss" (Table 2), defined as wt% solute in the solution after the quenching (note: this is material, which did not precipitate upon quenching and has to be taken into consideration in the further). The last row of Table 2 provides a minimum estimate of the solute content of this solution. It is also possible that the solute was still higher concentrated and some of the solute from the solution precipitated within the capsule upon piercing and drying. The determination of the absolute solute content in the aqueous fluid phase under run conditions following the procedure of STALDER et al. (2000) cannot be applied, as it is required that the fluid is separated into solid quench material and H_2O upon quenching.

The excess weight loss correlates well with temperature for both experimental series (Fig. 3a). If only the most alkaline analysis points (K/Al > 4) out of the outliers listed in Table 2 are considered, a fair correlation between excess weight loss and total solute measured by LAM-ICP-MS is obtained (Fig. 3b). The local chemistry of these points is probably highly influenced (or even dominated) by contamination of the solid quench by the highly alkaline solution that was observed after the run. The correlation of the last two rows presented in Table 2 suggests that the preliminary determined arbitrary units for the solute content of the fluid match the absolute solute content (Fig. 3b); it may even suggest that these points represent local portions of the trap, which hosted mainly the highly alkaline solution (i.e., the trap is heterogeneous on the scale of 100 μm), and the

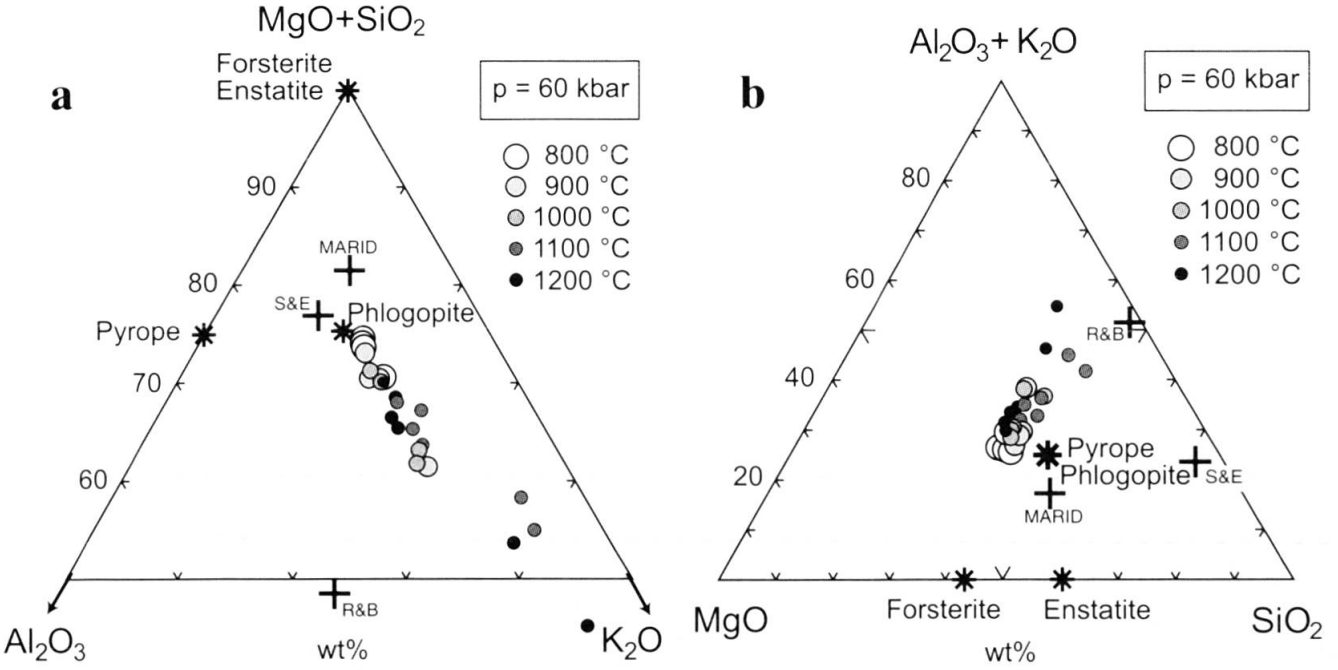

Fig. 1 Compositon of the dry solute in the run series phlogopite–H_2O at 60 kbar projected from H_2O: (a) $MgO+SiO_2 - Al_2O_3 - K_2O$ ternary diagram (wt%) and (b) $Al_2O_3+K_2O - MgO - SiO_2$ ternary diagram (wt%). Results from previous studies at 11 kbar and 1100 °C (R&B; RYABCHIKOV and BOETTCHER, 1980) and 20 kbar and 1100 °C (S&E; SCHNEIDER and EGGLER, 1986) are plotted for comparison. Between 10 and 20 kbar the silica contents in the fluid increases markedly (b), followed by an increase in MgO to 60 kbar. As the absolute solute content in the fluid (not shown in this figure) strongly increases between 20 and 60 kbar, the absolute silica contents in the fluid do not decrease. The approximate composition of a MARID-nodule (SWEENEY et al., 1993) is also shown (FeO was calculated as MgO). Except for the data at 20 kbar (S&E), which are too silica-rich, MARID could be produced by a reaction of forsterite+enstatite with a potassic fluid.

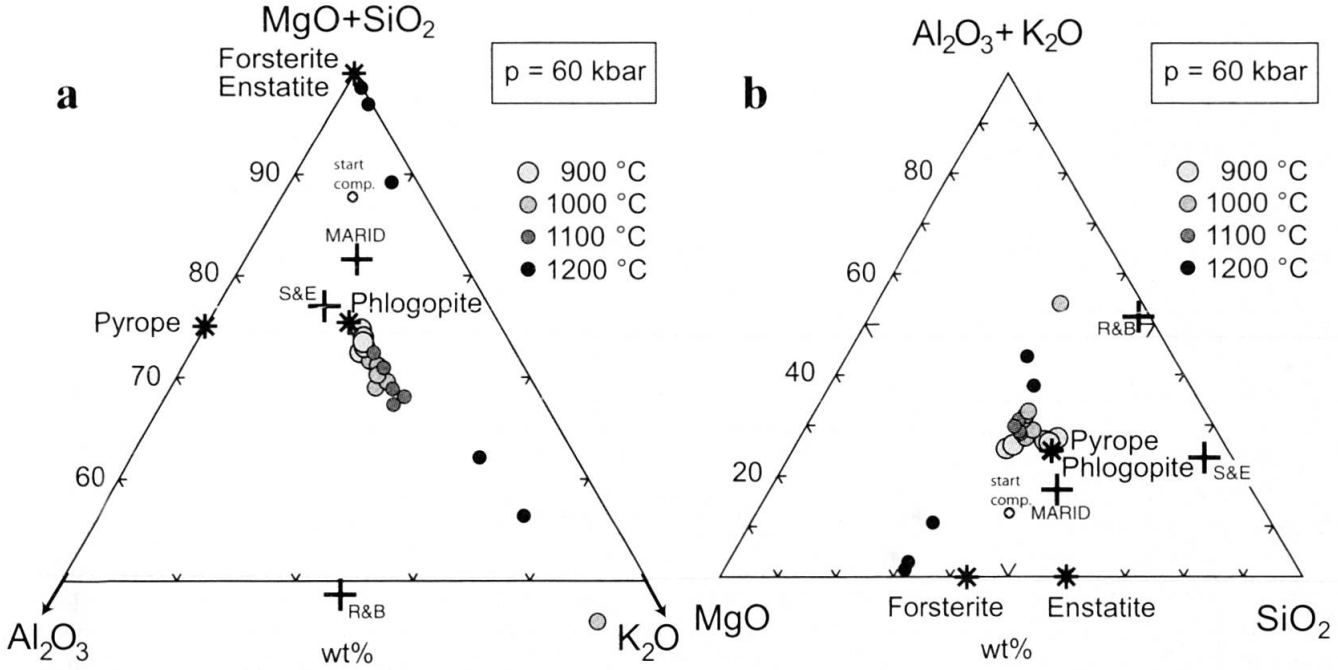

Fig. 2 Compositon of the dry solute in the run series forsterite–phlogopite–H_2O at 60 kbar: (a) $MgO+SiO_2 - Al_2O_3 - K_2O$ ternary diagram (wt%) and (b) $Al_2O_3+K_2O - MgO - SiO_2$ ternary diagram (wt%). For explanations see Fig. 1.

solute from the solution was precipitated between the diamond crystals during drying. If this interpretation is correct the second last row of Table 2 can be considered as wt% solute, which means that the solute contents in all runs were close to 50 wt% (Table 2). Figure 4 shows the amount of dissolved silicate for both series. For several runs two or three different data points are shown. Circles with the error bar give the solute content of the quench material with the phlogopite-like composition, and triangles show the solute content of the extraordinary K-rich quench. No obvious trend is visible for the phlogopite-like quench. In contrast, the K-rich quench shows a positive correlation between solute content and temperature, as observed for the excess weight loss (Fig. 3a).

The best estimate of the fluid compositions at run conditions is given by the chemographic presentation in Fig. 5. Two components have to be taken into account, the quench material with phlogopite-like composition and the highly alkaline solution. Figure 5 shows the approximate composition of the fluid phase (quadratic symbols), saturated with phlogopite, forsterite, garnet and enstatite, at 60 kbar and 900 °C and 1200 °C, respectively. Upon quenchimg the fluid separates into approximately 50 wt% phlogopite-like quench and 50 wt% K_2O+SiO_2-containing solutions (circles). The bulk solute (black dots) moves with increasing temperature from a composition close to phlogopite towards higher K_2O and SiO_2-contents. Table 3 shows the resulting modal propor-

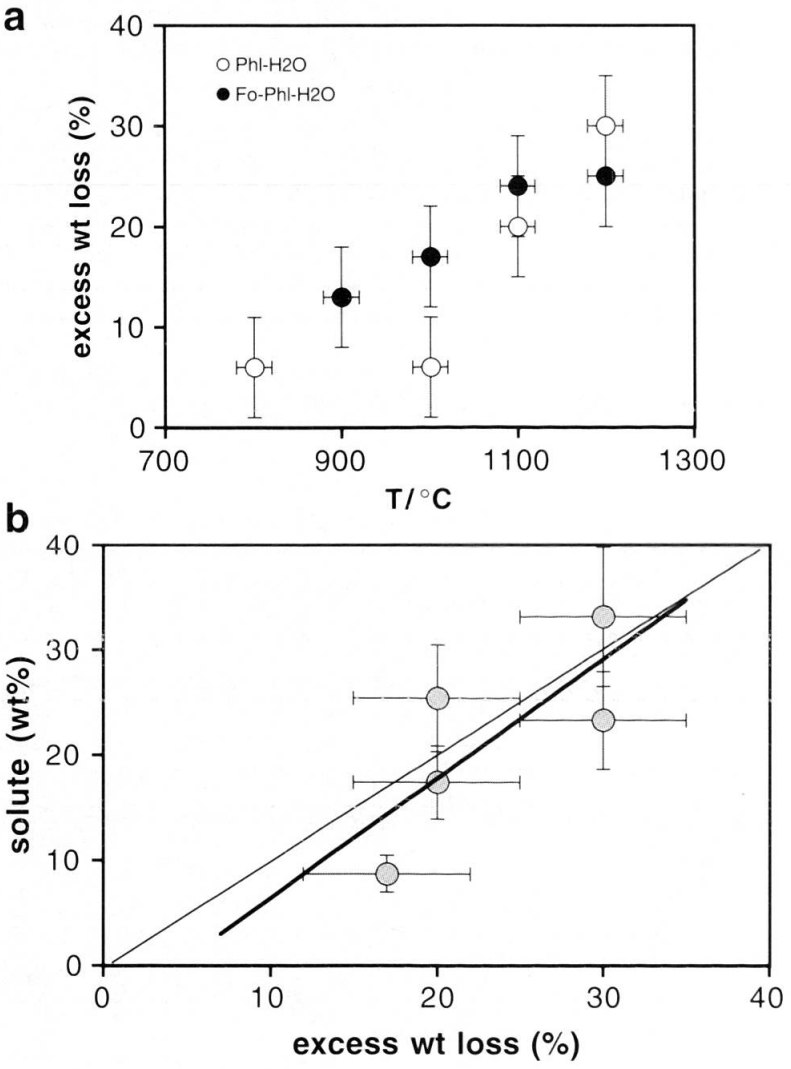

Fig. 3 During quenching not all solute was precipitated and considerable amounts of K_2O and SiO_2 stayed in an alkaline solution. The release of this solution after the run lead to a weight loss that was higher than the initial water content of the charge. (a) The amount of solute in the solution is dependent on temperature. (b) In several runs single measured points (local portions of the diamond trap) exhibited a chemical composition very different from most other data points. The absolute content of precipitated material of these local portions of the trap correlates (thick line, $R^2 = 0.6$) with the excess weight loss of the given run. The thin line (excess weight loss = solute content) is shown for comparison. Error bars are estimated.

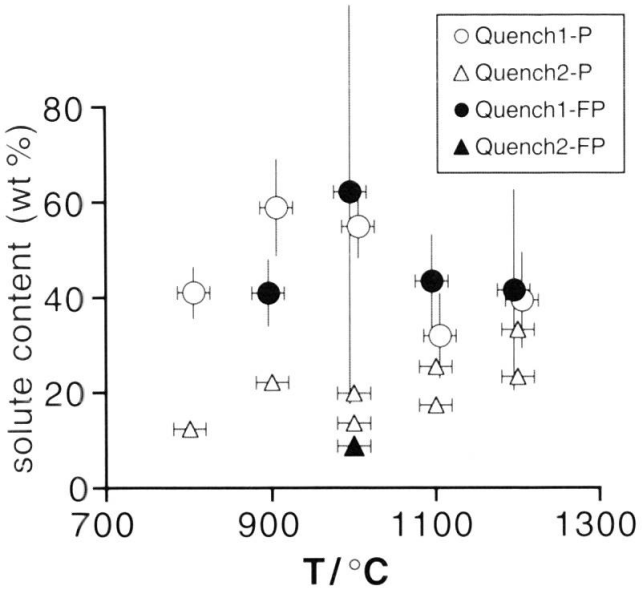

Fig. 4 Solute contents in the fluids at various temperatures (arbitrary units) in the system forsterite–phlogopite–water (filled symbols) and phlogopite–water (open symbols). The solute content for the phlogopite-dominated quench (circles) is approximately 50 wt%. Triangles represent single analyses of extremely K-rich and MgO- and Al_2O_3-poor data points (Table 2).

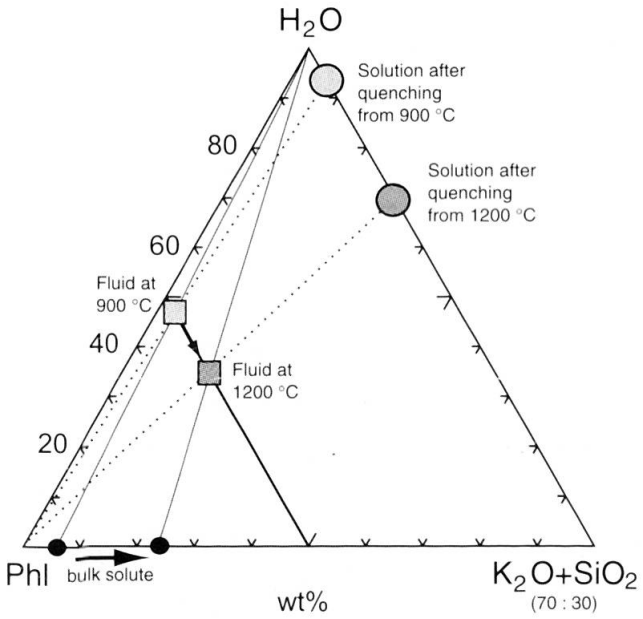

Fig. 5 Chemographic presentation of the fluid compositions at run condition within the series forsterite–phlogopite–H_2O. Fluid compositions likely represent a mixture of phlogopite-like quench and a K-Si-rich solution (nearly in equal proportions). The estimated solvent contents in the solution after quenching (big circles) are derived from Table 2 (last row). The solute content in the fluid (quadratic symbols) increases slightly with increasing temperature (from 50 to about 60 wt%), and the bulk solute is shifted systematically towards higher K_2O and SiO_2 concentrations (arrows).

tions (calculated by mass balance) of the runs at temperatures close to the disappearance of phlogopite in the system forsterite – phlogopite – water, and the modal proportion in the initially Fo-free system for comparison. Up to the disappearance of phlogopite, the main difference between the two starting compositions is the modal amount of forsterite and phlogopite. In other words, adding of forsterite to the starting composition did not change the buffering phase assemblage, which is reflected by the similar results of both run series.

4. Discussion

The observation that runs varying from 900–1100 °C show very similar results for both series (with and without initial forsterite), suggests that forsterite was formed upon phlogopite dissolution and both run series were buffered by the same phase assemblage. This point is strengthened by the occurrence of minor amounts of forsterite in some of the initially forsterite free runs. The high amount of MgO in the fluid in the system forsterite–phlogopite–H_2O at 1200 °C indicates melting of the forsterite component, as melting of pure forsterite in the system forsterite–H_2O is expected to occur at this temperature (INOUE, 1994).

Due to several reasons the solute content in the fluid determined in this study is considerably more uncertain than data from previous studies using the same method (STALDER et al., 2000, 2001). Firstly, not all solute precipitated during quenching (actually a prerequisite of the technique); secondly, these sets of experiments could not be calibrated or checked with a run of a similar composition with known solute content. In our previous studies the solute contents varied between a few and nearly 100 wt% within one set of experiments, setting an internal control of the scale. This was also aimed in this study by varying the temperature between 800 and 1200 °C, but in

Table 3 Modal compositions according to mass balance.

Phl – H_2O	Fo – Phl – H_2O		
1200 °C	1100 °C	1200 °C	
6	47	≈ 40	wt% Forsterite
3	3		wt% Enstatite *
16	12	≈ 20	wt% Pyrope *
40	2		wt% Phlogopite
35	36	≈ 40	wt% Fluid/Melt

* pure end-members were considered; at ambient conditions <2 mol% Pyr in Opx and En in Gt is dissolved (FEI and BERTKA, 1999).

contrary to our previous studies, the contrast between low and high solubility with increasing temperature was not revealed here. Owing to these shortcomings the results presented here should mainly be regarded relative to each other (i.e., element ratios, trends), but could be considered being correct within a factor of two (even if most data points show a much better precision). The monotonous composition of the fluid phase between 800 and 1200 °C is in accord to experiments in the Ti–KNCMASH system, where no significant changes in quench texture were observed between 1000 and 1400 °C (KONZETT, 1997).

Since the total amount of solute could not be accurately determined, it cannot be answered unequivocally whether the investigated systems reached its second critical endpoint. The high amount of solute in the fluid and the low variation of the fluid chemistry over several hundred degrees are features, which usually occur in simpler silicate–H_2O systems, as a second critical endpoint (i.e. the termination of the solidus) is reached. However, results of KMASH13 could be interpreted as two different, immiscible fluids or melts. One of them is a hydrous forsteritic melt, consisting of two thirds forsterite component and one third H_2O; the second fluid is highly potassic. It is also possible, that both were one homogeneous phase at run conditions and unmixed and separated during quenching, even if this explanation is less favourable. To answer this question, in-situ observations in a Bassett-cell (SHEN and KEPPLER, 1997) have to be carried out. However, 60 kbar and 1200 °C are currently beyond the limits of that experimental technique.

The critical end-point on the hydrous mantle solidus is estimated to occur between 30 and 80 kbar (RYABCHIKOV, 1993; WYLLIE and RYABCHIKOV, 2000). To compare the KMASH system with the Earth's mantle, further components (in particular FeO, CaO and CO_2) have to be taken into account. The addition of FeO and CaO is expected to enhance the amount of solute in the fluid at given pressure and temperature; furthermore, the solidus temperature (as long as it is defined and the second critical endpoint is not reached) is shifted towards lower temperatures. This results in lower solubility of silicate material in the fluid at the solidus. On the other hand lowers CO_2 the solute content in the fluid (EGGLER and ROSENHAUER, 1978; SCHNEIDER and EGGLER, 1986) and shifts the second critical endpoint to higher pressures. Therefore it is not clear, whether the termination of the solidus in the KMASH system occurs at higher or lower pressures than 60 kbar. Both interpretations are not in conflict with the results from the natural lherzolite–H_2O system and KMASH.

Comparison with previous quantitative studies has to consider that none of them was buffered in all components. Previous experimental investigations at 11 kbar and 1100 °C (RYABCHIKOV and BOETTCHER, 1980) exhibit incongruent dissolution of phlogopite, leaving forsterite as a residual phase (Fig. 1). The total amount of solute was approximately 14 wt%. The Mg-solubility at these conditions is negligible (MODRESKI and BOETTCHER, 1973). For runs up to 30 kbar (RYABCHIKOV and BOETTCHER, 1980) the exact composition of the fluid was not quantified, but much higher K-solubilities and abundant quench phlogopite was observed. It was therefore concluded that the Mg-solubility increases with increasing pressure. Experiments on a phlogopite lherzolite at 20 kbar and 1100 °C showed that the aqueous fluid is much richer in silica, but still dissolves only minor amounts of MgO (SCHNEIDER and EGGLER, 1986). The total amount of solute was between 10 and 16 wt%.

The results of our study show that the trend of increasing Mg-solubility (RYABCHIKOV and BOETTCHER, 1980) continues to 60 kbar. An increase of the Mg/Si-ratio in the fluid with increasing pressure has also been observed in the system MgO–SiO_2–H_2O. Up to 30 kbar the solute is dominated by silica with only minor amounts of MgO (NAKAMURA and KUSHURO, 1974; RYABCHIKOV et al., 1982), whereas results at 90 kbar reveal that MgO is more soluble than SiO_2 (STALDER et al., 2001). These experimental evidences are in accord with diamondiferous xenoliths from Udachnaya/Yakutia (SOBOLEV et al., 1999), which exhibit depletions in SiO_2 and enrichment in MgO upon metasomatic overprint.

5. Petrological application

The results presented above have only limited relevance for the generation of potassic and ultrapotassic magmas because important components in their source regions, e.g., CaO, CO_2 and fluorine (FOLEY et al., 1986; FOLEY, 1992; MELZER and FOLEY, 2000), were not considered in our study. The fluids have thus not been saturated with clinopyroxene, a major constituent of the source region of ultrapotassic rocks (CARMICHAEL, 1967; FOLEY, 1992). However, MARIDs (Mica–Amphibole–Rutile–Ilmenite–Diopside assemblages) contain no F, and experimental evidence (SWEENEY et al., 1993; SWEENEY, 1994) implies that the presence of CO_2 is not compatible with K-richterite at all, and that CO_2 does not play a significant role in the formation of MARIDs and PKPs (phlogopite–K-richterite peridotites). The present work extends

the current data set on fluid compositions in K-bearing systems to much higher pressures. The increasing amount of MgO-dissolution (i.e. approaching congruent dissolution of phlogopite) with enhanced pressure demonstrates that extrapolations of solubilities from runs at lower pressures (RYABCHIKOV and BOETTCHER, 1980) have to be regarded with caution. The enhanced MgO-solubility in the fluid (as well as the higher MgO-content in the hydrous melt with increasing pressure (INOUE, 1994; STALDER et al., 2001) implies that the phase topology in peridotitic systems changes significantly between 30 and 60 kbar. Following the hybridisation model of SEKINE and WYLLIE (1980), some reactions should be formulated differently, e.g., the eutectic occurs between forsterite and enstatite (instead of enstatite and quartz), and phlogopite dissolution/melting may become nearly congruent at pressures still higher than 60 kbar. An aqueous fluid liberated from a subducted slab is able to dissolve high amounts of potassium, but – in contact with the basaltic portion and the sediment cover – will be initially poor in magnesium. If such an H_2O-dominated fluid is released into the peridotitic mantle wedge, it may react with forsterite to form enstatite. The solute in the fluid will then be dominated by a phlogopitic component, which can be transported by this aqueous fluid. Phlogopite crystallisation (i.e. modal K-metasomatism) is expected to occur with decreasing pressure and/or temperature (e.g., in a cratonic region forming beneath a continental root). The solute determined experimentally mixed with forsterite and enstatite resembles the chemical composition of MARID (Fig. 1). This allows the interpretation that MARIDs may form by a reaction between K-rich aqueous fluids and peridotite (SWEENEY et al., 1993).

The influence of CO_2 on the solute in the fluid is not very well established. On the one hand results from SCHNEIDER and EGGLER (1986) may suggest that CO_2 strongly reduces the amount of solute at 20 kbar (but this observation is based on a single experiment), on the other hand fluid inclusions from natural diamonds reveal higher solubilities of MgO and K_2O in the CO_2-richer fluids than in the H_2O-dominated ones (SCHRAUDER and NAVON, 1994).

Acknowledgements

This project was kindly supported by the Schweizer Nationalfond, grant 2000-050661.97. Sven Girsperger is thanked for helping with the hydrothermal syntheses. Constructive reviews by Christoph Hauzenberger and an anonymous reviewer are gratefully acknowledged.

References

AOKI, K.I. (1975): Origin of phlogopite and potassic richterite bearing peridotite xenoliths from South Africa. Contrib. Mineral. Petrol. 53, 145–156.

CARMICHAEL, I.S.E. (1967): The mineralogy and petrology of the volcanic rocks from the Leucite Hills, Wyoming. Contrib. Mineral. Petrol. 15, 24–66.

DAWSON, J.B. and SMITH, J.V. (1977): The MARID (mica-amphibole-rutile-ilmenite-diopside) suite of xenoliths in kimberlite. Geochim. Cosmochim. Acta 41, 309–323.

EGGLER, D.H. and ROSENHAUER, M. (1978): CO_2 in silicate melts: II. Solubilities of CO_2 and H_2O in $CaMgSi_2O_6$ (diopside) liquids and vapours at pressures to 40 kbar. Am. J. Sci. 278, 64–94.

ERLANK, A.J., WATERS, F.G., HAWKESWORTH, C.J., HAGGERTY, S.E., ALLSOPP, H.L., RICKARD, R.S. and MENZIES, M.A. (1987): Evidence for mantle metasomatism in peridotite nodules from Kimberley pipes, South Africa. In: MENZIES, M.A. and HAWKESWORTH, C.J. (eds.): Mantle Metasomatism, Academic Press Inc., London, 221–311.

FEI, Y. and BERTKA, C.M. (1999): Phase transition in the Earth's mantle and mantle mineralogy. In: FEI, Y., BERTKA, C.M. & MYSEN, B., (eds.): Mantle petrology: Field observations and high pressure experimentation, Geochemical Society, Special Publication No. 6, 189–207.

FOLEY, S.F. (1992): Petrological characterization of the source components of potassic magmas: geochemical and experimental constraints. Lithos 28, 187–204.

FOLEY, S.F., TAYLOR, W.R. and GREEN, D.H. (1986): The effect of fluorine on phase relationships in the system $KAlSiO_4$ – Mg_2SiO_4 – SiO_2 at 28 kbar and the solution mechanism of fluorine in silicate melts. Contrib. Mineral. Petrol. 93, 46–55.

GÜNTHER, D., FRISCHKNECHT, R. and HEINRICH, C.A. (1997): Capabilities of a 193 nm ArF excimer laser for LA-ICP-MS micro analysis of geological materials. J. Anal. At. Spectrom. 12, 939–944.

HATTENDORF, B. and GÜNTHER, D. (2000): Characteristics and capabilities of an ICP-MS with a dynamic reaction cell for dry aerosols and laser ablation. J. Anal. At. Spectrom. 15, 1125–1131.

INOUE, T. (1994): Effect of water on melting phase relations and melt compositions in the system Mg_2SiO_4-$MgSiO_3$-H_2O up to 15 GPa. Phys. Earth. Planet. Int. 85, 237–263.

KONZETT, J. (1997): Phase relations and chemistry of Ti-rich K-richterite-bearing mantle assemblages: an experimental study to 8.0 GPa in a Ti-KNCMASH system. Contrib. Mineral. Petrol. 128, 385–404.

LONGERICH, H.P., JACKSON, S.E. and GÜNTHER, D. (1996): Laser Ablation Inductively Coupled Plasma Mass Spectrometry Transient Signal Data Acquisition and Analyte Concentration Calculation. J. Anal. At. Spectrom. 11, 899–904.

MELZER, S. and FOLEY, S.F. (2000): Phase relations and fractionation sequences in potassic magma series modelled in the system $CaMgSi_2O_6$ – $KAlSiO_4$ – Mg_2SiO_4 – SiO_2 – F_2O_{-1} at 1 bar to 18 kbar. Contrib. Mineral. Petrol. 138, 186–197.

MODRESKI, P.J. and BOETTCHER, A.L. (1972): The stability of phlogopite + enstatite at high pressures: a model for micas in the interior of the Earth. Am. J. Sci. 272, 852–869.

MODRESKI, P.J. and BOETTCHER, A.L. (1973): Phase relationships of phlogopite in the system K_2O-MgO-CaO-Al_2O_3-SiO_2-H_2O to 35 kilobars: a better model

for micas in the interior of the Earth. Am. J. Sci. 273, 385–414.

NAKAMURA, Y. and KUSHIRO, I. (1974): Composition of the gas phase in Mg_2SiO_4-SiO_2-H_2O at 15 kbar. Carn. Inst. Wash. Yb. 73, 255–258.

RYABCHIKOV, I.D. (1993): Fluid transport of ore metals in ultramafic mantle rocks. Proceedings of the Eighth Quadrennial IAGOD Symposium, 425–433.

RYABCHIKOV, I.D. and BOETTCHER, A.L. (1980): Experimental evidence at high pressure for the potassic metasomatism in the mantle of the Earth. Am. Mineral. 65, 915–919.

RYABCHIKOV, I.D., SCHREYER, W. and ABRAHAM, K. (1982): Compositions of aqueous fluids in equilibrium with pyroxenes and olivines at mantle pressures and temperatures. Contrib. Mineral. Petrol. 79, 80–84.

SATO, K., KATSURA, T. and ITO, E. (1997): Phase relations of natural phlogopite with and without enstatite up to 8 GPa: implications for mantle metasomatism. Earth Planet. Sci. Lett. 146, 511–526.

SCHNEIDER, M.E. and EGGLER, D.H. (1986): Fluids in equilibrium with peridotite minerals: implications for mantle metasomatism. Geochim. Cosmochim. Acta 50, 711–724.

SCHRAUDER, M. and NAVON, O. (1994): Hydrous and carbonatitic mantle fluids in fibrous diamonds from Jwaneng, Botswana. Geochim. Cosmochim. Acta 58, 761–771.

SEKINE, T. and WYLLIE, P.J. (1980): Phase relationships in the system $KAlSiO_4$ – Mg_2SiO_4 – SiO_2 – H_2O as a model for hybridisation between hydrous siliceous melts and peridotite. Contrib. Mineral. Petrol. 79, 368–374.

SHEN, A.H. and KEPPLER, H. (1997): Direct observation of complete miscibility in the albite–H_2O system. Nature 385, 710–712.

SOBOLEV, V.N., TAYLOR, L.A., SNYDER, G.A., JERDE, E.A., NEAL and C.R., SOBOLEV, N.V. (1999): Quantifying the effects of metasomatism in mantle xenoliths: constraints from secondary chemistry and mineralogy in udachnaya eclogites, Yakutia. Int. Geol. Rev. 41, 391–416.

STALDER, R., ULMER, P., THOMPSON, A.B. and GÜNTHER, D. (2000): Experimental approach to constrain second critical endpoints in fluid/silicate systems: near-solidus fluids and melts in the system albite-H_2O. Am. Mineral. 85, 68–77.

STALDER, R., ULMER, P., THOMPSON, A.B. and GÜNTHER, D. (2001): High pressure fluids in the system MgO-SiO_2-H_2O under upper mantle conditions. Contrib. Mineral. Petrol. 140, 607–618.

SWEENEY, R.J. (1994): Carbonatite melt compositions in the Earth's mantle. Earth Planet. Sci. Lett. 128, 259–270.

SWEENEY, R.J., THOMPSON, A.B. and ULMER, P. (1993): Phase relations of a natural MARID composition and implications for MARID genesis, lithospheric melting and mantle metasomatism. Contrib. Mineral. Petrol. 115, 225–241.

WATERS, F.G. and ERLANK, A.J. (1988): Assessment of the vertical extent and distribution of mantle metasomatism below Kimberley, South Africa. J. Petrol., Special Lithosphere Issue, 185–204.

WENDLANDT, R.F. and EGGLER, D.H. (1980): The origins of potassic magmas: 2. Stability of phlogopite in natural spinel lherzolite and in the system $KAlSiO_4$-MgO-SiO_2-H_2O-CO_2 at high pressures and high temperatures. Am. J. Sci. 280, 421–458.

WYLLIE, P.J. and RYABCHIKOV, I.D. (2000): Volatile components, magmas, and critical fluids in upwelling mantle. J. Petrol. 41, 1195–1206.

YODER, H.S.Jr. and KUSHIRO, I. (1969): Melting of a hydrous phase: phlogopite. Am. J. Sci. 267A, 558–582.

Manuscript received May 15, 2001 ; revision accepted February 8, 2002.